Original Paper

Atomic force microscope study of the topography of float glasses and a model to explain the bloom effect

Doris Moseler[1)], Gerhard Heide and Günther Heinz Frischat

Institut für Nichtmetallische Werkstoffe (Professur für Glas), Technische Universität Clausthal, Clausthal-Zellerfeld (Germany)

The topography and nanostructure of several technical borofloat and soda-lime-silicate float glasses were investigated by a high-resolution atomic force microscope (AFM). The irregular ripple pattern to be seen on as-received atmosphere and tin bath side surfaces had an average diameter of ≈ 60 nm, heights < 1 nm and root mean square (rms) roughnesses on (1 × 1) μm² images of < 0.25 nm. Topographies obtained in the mirror region of fracture surfaces displayed a somewhat coarser nanostructure. It could further be assured that there are no specific differences between the interior and the edge of the float glass sample. Inhomogeneities like precipitates, crystals, phase separation or pores are not caused by the in-diffusion of tin into the float glass. After annealing the float glasses in air, several of them showed the already long known phenomenon of bloom, a greyish haze produced by a wrinkling of the tin bath glass surface. The borofloat glasses did not produce bloom under any condition. The same was true for the Fe_2O_3-rich green and blue glasses. Depending on sample dimensions and annealing conditions only the Fe_2O_3-poor clear float glasses developed a pronounced bloom effect. It is known that annealing of the glasses in air causes an oxidation of Sn^{2+} to Sn^{4+}, which acts as a network former. This causes a change in glass properties near the surface. However, the precisely measured in-depth profiles of all relevant species in the nanometer and the micrometer regions of the float glasses showed that only in the case of the Fe_2O_3-poor silicate float glasses a reversed Sn^{2+} diffusion from the interior to the surface is caused by the air annealing, forming a very high and steep tin (Sn^{4+}) enrichment in a superficial layer with a thickness between 50 and 150 nm.

In analogy to thin film technology a simplified model was developed and a free buckling length of ≈ 2.3 μm was estimated for the bloom surface, which is in reasonable agreement with the experimental finding. It was further shown that a sol-gel derived SiO_2 coating of the bloom surface could enhance the optical transmission of the glass considerably.

1. Introduction

Float glasses are produced world-wide in huge amounts and are among the most important technical glasses. They are prepared by floating silicate or borosilicate glass melts on a tin melt in a specially designed float chamber. Float glasses have two quite dissimilar sides. At the tin bath side the performance of the glass surface is mainly determined by the tin ions which have diffused into the glass in contact with the molten tin. At the atmosphere side, on the other hand, the surface is melt-formed (fire-polished) and displays pristine nature. Of course, both sides can be altered during further handling and/or storage.

Received 14 November 2001, revised manuscript 13 February 2002.

Presented in German at the autumn session of Technical Committee I of the German Society of Glass Technology (DGG) in Würzburg(Germany) on 13 October 1999, and at the 75th Annual Meeting of the DGG in Wernigerode (Germany) on 22 May 2001.

[1)] Now with: Schott Glas, Mainz (Germany).

During recent years the interaction of float glass melts with the tin bath melt has been studied extensively especially with regard to questions how the tin penetrates the glass melt, how the glass properties are changed, and which is the origin of the anomalous tin hump several micrometers below the glass surface, e. g. [1 to 7]. A further consequence of the tin penetration can result in the phenomenon of bloom, a greyish haze which occurs on several glasses after reheating. It has been shown that this haze is produced by a microscopic wrinkling of the tin bath surface of the glass, obviously related to the oxidation of Sn^{2+} to Sn^{4+} [8 and 9].

It was the aim of this work to carefully study possible changes in topography and nanostructure which occur as a consequence of the glass tin interaction. Some glasses were fractured to be able to find the possible formation of precipitates, phase separation, crystals or pores in the zone of the glass where the tin has diffused in. Bloom was investigated as a function of parameters like glass composition, sample dimensions and heating program. The influence of a thin sol-gel layer was stud-

Table 1. Some analytical aspects of the commercial float glasses investigated

	OW0017	OF0115	D0130	OG0605	V1800	BG0560	BF0022	BF0020
Fe_2O_3 in wt%	0.017	0.115	0.13	0.605	1.80	0.560	0.022	0.020
SO_3 in wt%	0.239	0.228		0.188	0.22	0.005	0.001	0.001
$\frac{Fe^{2+}}{Fe^{2+}+Fe^{3+}}$ in %	33.2	24.2		23.9	26.1	60.0		

ied, too. A high resolution atomic force microscope (AFM) was applied for these investigations.

2. Experimental

2.1 Samples

Eight commercial float glasses with a thickness of 4 mm were investigated. Six of them were soda-lime silicate float glasses with Fe_2O_3 contents ranging from 0.017 to 1.80 wt% and the two others were floated borosilicate glasses having Fe_2O_3 contents of ≈ 0.02 wt%, see table 1. The samples were cleaned by brushing them with a nylon brush in hot water with mild surfactants and rinsed with deionized water. After that the samples were further cleaned for 5 min in an ultrasonic bath with ethanol. To prepare fresh fracture surfaces the float glass sheets were cut into strips of 8 mm width, notched by sawing them gently and fractured perpendicularly to their length. These samples were stored in a desiccator. To produce samples which distinctly show the bloom effect, glass pieces with differing dimensions between (5 × 5) mm^2 and (100 × 100) mm^2 were annealed in air at 650 to 690 °C with holding times between 0 and 1 h. Heating rates were 10 K/min.

To investigate the influence of a sol-gel coating on a sample which displays a distinct bloom effect, a clear float glass (0.13 wt% Fe_2O_3) was heated first to 670 °C for 1 h. After cooling the glass sample was dipcoated in a solution of tetraethoxysilane, ethanol, H_2O, and 1 mol/l HNO_3 [10] with an oxide content of 6.5 %. An SiO_2 layer of ≈ 100 nm thickness was then achieved by heating the coated sample to 500 °C.

2.2 Methods of analysis

The topographies of the float glass samples prepared as above were investigated using a Nanoscope II atomic force microscope (Digital Instruments, Santa Barbara, CA, USA) with a maximum scan size of (100 × 100) μm^2 and maximum heights in the z-axis of ≈ 6 µm. The contact mode was applied. Si_3N_4 and silicon tips (Digital Instruments) were used as sensors. The Si_3N_4 tips have nominal spring constants of ≈ 0.12 N/m and those of the silicon tips are between 0.02 and 0.1 N/m. Flat samples were fixed on a sample holder with a double-sided adhesive tape, non-flat samples were embedded in plasticine with the surface of interest parallel to the scanning plane. The lateral resolution achievable on these glass surfaces is ≈ 5 nm [11].

Tin in-depth profiles were recorded on different float glasses by using the secondary neutral mass spectrometry method (SNMS). An INA 3 apparatus (Leybold AG, Köln, Germany), working in the high frequency mode (Specs GmbH, Berlin, Germany), was used. Details of this technique can be found in [12].

Optical transmission spectra were recorded with an OMEGA spectrophotometer (Bruins Instruments, Puchheim, Germany).

3. Results and discussion

3.1 Topography of as-received and fracture surfaces

Figures 1a and b display typical AFM images of the atmosphere side (a) and the tin bath side surfaces (b), respectively. The patterns to be seen consist of irregular ripples with diameters between 10 and 100 nm, on an average of ≈ 60 nm. The height of the ripples is <1 nm, some of them are twice as high as the others. The (1 × 1) μm^2 rms (root mean square) roughness (all recorded rms roughnesses are related to this scan area) of the atmosphere side surface is ≈ 0.25 nm, a little larger than that of the tin bath surface with 0.15 to 0.20 nm. The surfaces of the borofloat glasses are a little smoother than those of the soda-lime float glasses. Altogether, the ripple patterns found are in line with earlier results [11].

Of course, both the atmosphere and the tin bath side surfaces display sporadically also particles, dendritically grown crusts, wiping tracks and/or indentations from glass fragments or crystals. These particles and crusts are not typical and can partly also be moved on the surface by the scanning tip. They are probably haze and corrosion products [1 and 13].

The AFM images of figures 2a to d show for comparison four different fracture surfaces. All images were taken in the fracture mirror, the smoothest part of the fracture surface [14]. In figure 2a a typical example of a soda-lime float glass fracture surface from the interior

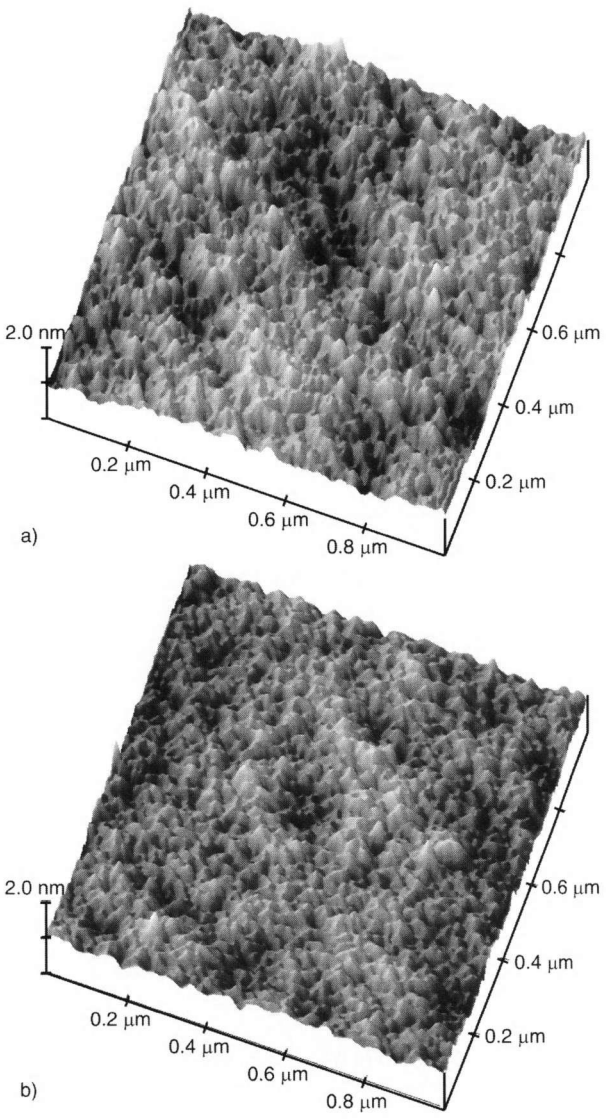

Figures 1a and b. AFM height mode images of as-received float glass surfaces; a) atmosphere side, b) tin bath side.

of the glass is to be seen. The diameters of the ripples are between 80 and 140 nm and their heights lie between 1 and 2 nm. The rms roughnesses amount to 0.6 to 0.8 nm and are 3 to 4 times higher than those of the as-received surfaces. There are also better resolved images with ripple diameters of 60 to 80 nm. Figure 2b shows the image of the fracture surface of a borofloat glass. The dimensions are similar as before with ripple diameters between 50 to 80 nm and ripple heights of 1 to 2 nm.

Figure 2c displays an AFM image of the fracture surface at the edge of the sample to the tin bath side. The ripples have diameters between 50 to 80 nm and their maximum heights amount to 2.5 nm. From figures 2a and c one can conclude that the glass investigated is equally homogeneous not only in its interior but also at the edge and inhomogeneities like precipitates, phase separation, crystals or pores are not caused by the in-diffusion of the tin into the float glass. It is a general finding that the glass ripple patterns imaged on fracture surfaces do not show specific differences between the interior and the edge of float glass samples, irrespective which type of glass is investigated. For comparison figure 2d displays an AFM image of a fracture surface of the commercial product with trade name K-glass, whose heat-insulating effect stems from a mostly crystalline SnO_2 coating $\approx$ 350 nm thick, on the float glass. Such a coating is clearly distinguished from the adjacent glass ripple pattern. Recently small SnO_2 precipitates ($\approx$ 1 nm in diameter) have been reported to be present near the very surface of float glass (tin bath side) after annealing it under oxidizing conditions [15]. This phase separation process was caused by Sn^{2+} diffusion from the interior of the glass to the surface, which did not occur during annealing in argon atmosphere. Such precipitates are too small to be detectable by an air-operated AFM [11].

Figure 3 shows a series of AFM images of a fracture surface of a float glass sample with a sequence of inhomogeneities. The tin bath side is at the right hand side. Near the tin bath surface a region with gross inhomogeneities, each of them with a diameter of 250 to 400 nm and $\approx$ 55 nm height, can be seen. The rms roughness of this area is $\approx$ 13.5 nm. Going further into the interior of the sample, one finds at a depth of 10 to 15 μm a large number of smaller inhomogeneities, see the respective (5×5) μm^2 magnified images. Their diameters lie between 150 to 200 nm and their heights are $\approx$ 5 nm. The rms roughness is $\approx$ 2.1 nm. At a depth of about 20 μm most of the inhomogeneities to be seen reach the sizes of the glass ripple pattern and can only be distinguished from it because of their more distinct shapes. Their rms roughness of 0.94 nm is only a little higher than that of the surrounding glass ripple pattern with 0.77 nm. Inhomogeneities like those shown in figure 3 occur sporadically also on fracture surfaces of other float glass samples, near the edges of both the tin bath and the atmosphere sides and also in the interior of the glass samples. They obviously do not result from an interaction between the glass melt and the tin melt. To learn more about their origin further specific work is necessary.

Freshly prepared float glass fracture surfaces react within minutes e. g. with the water vapor of the air. Thus also some typical corrosion products were found, similar to those obtained after specific corrosion experiments in moist atmospheres or in aqueous solutions [13, 16 to 18].

Glass surfaces inspected with an AFM are never totally smooth, although the method is capable to image smooth parts on distinct crystal surfaces [11]. Rädlein [11 and 19] and also Gupta et al. [20] discussed the origin of this nanoscale roughness. Gupta et al. [20] proposed that the minimum observed nanoscale roughness of a pristine melt-formed surface is controlled by the surface tension at the glass transition temperature T_g and that the roughness in the mirror region of a fracture surface reflects the intrinsic inhomogeneities in the

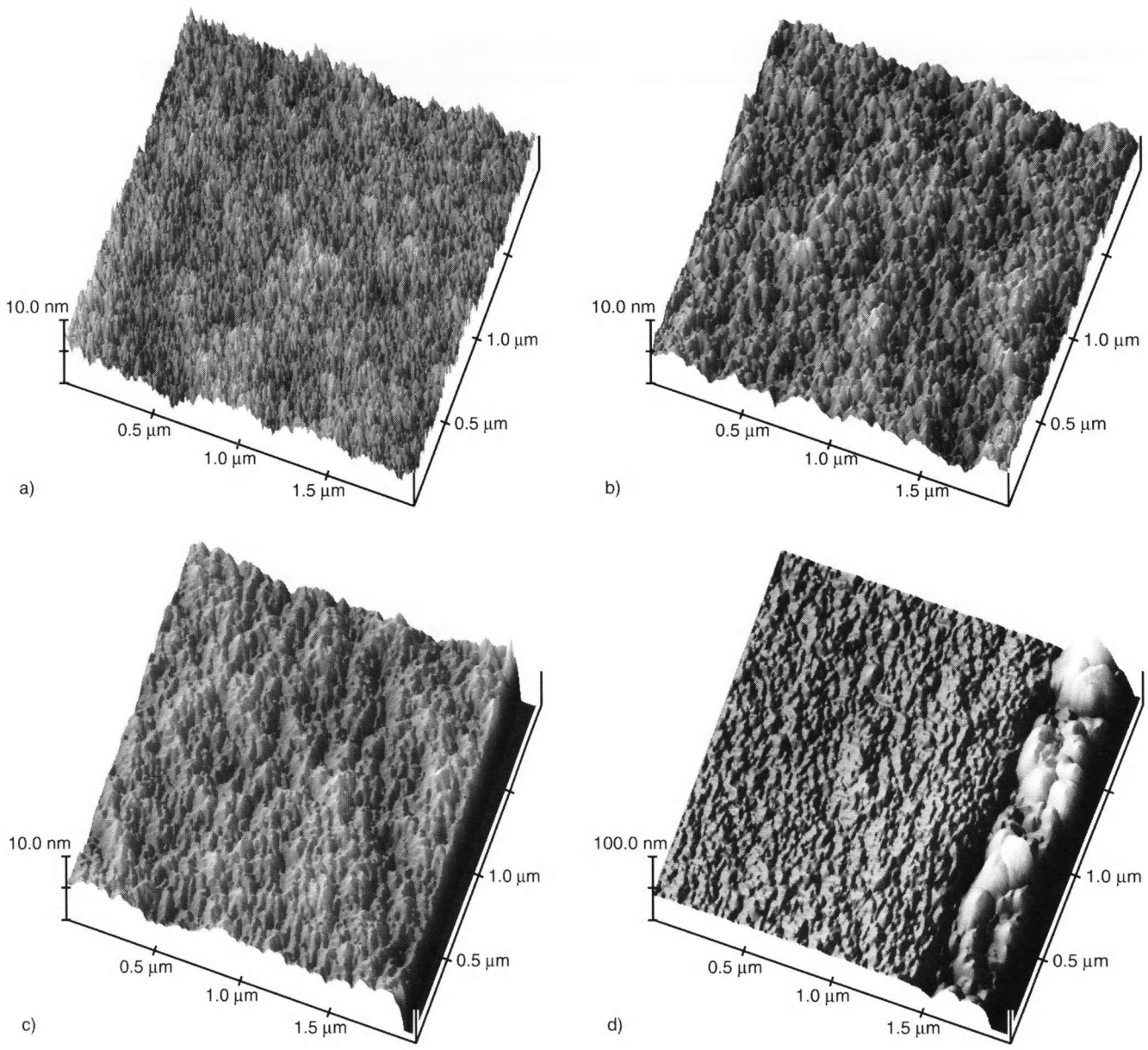

Figures 2a to d. AFM height mode images of fractured float glass surfaces; a) glass V1800 (interior), b) borofloat glass, c) glass V1800 (edge at the tin bath side), d) commercial heat insulating K-glass at the edge to its crystalline SnO_2 coating.

structure of the glass. According to Rädlein [11 and 19], who also listed the results obtained so far on a variety of different glasses by different authors, further reasons might be responsible for the glass ripple pattern observed. One model, explaining the occurrence of a ripple pattern, can be related to a nonuniform absorption of OH groups at the glass surface [19]. This model was developed initially for silica glass but it may equally be valid for other oxide glasses. Glass surfaces may contain hydrophilic and hydrophobic regions. Hydrophilic regions absorb OH groups and these then adsorb H_2O molecules via hydrogen bridges. Hydrophobic regions do not react either with OH groups or with water molecules. The scanning tip thus finds these dissimilar regions and images a ripple pattern. An estimation displays that the diameters of these ripples, "seen" by the tip, can be ≈50 nm, in close agreement with the experimental findings [19]. Of course, further explanations may also be valid for the glass ripple pattern.

Rädlein et al. [21] found ridges at the edges of a float glass fracture surface at the tin bath side. Similar ridges have been found occasionally also during this work both at the tin bath and the atmosphere sides of the glass. They obviously can be interpreted as a fracture phenomenon.

3.2 Topography of bloom surfaces

As already mentioned, the phenomenon of bloom is obviously related to the oxidation of Sn^{2+} to Sn^{4+} during reheating of float glasses in air, whose "tin count" (determined by X-ray fluorescence spectrometry) is higher

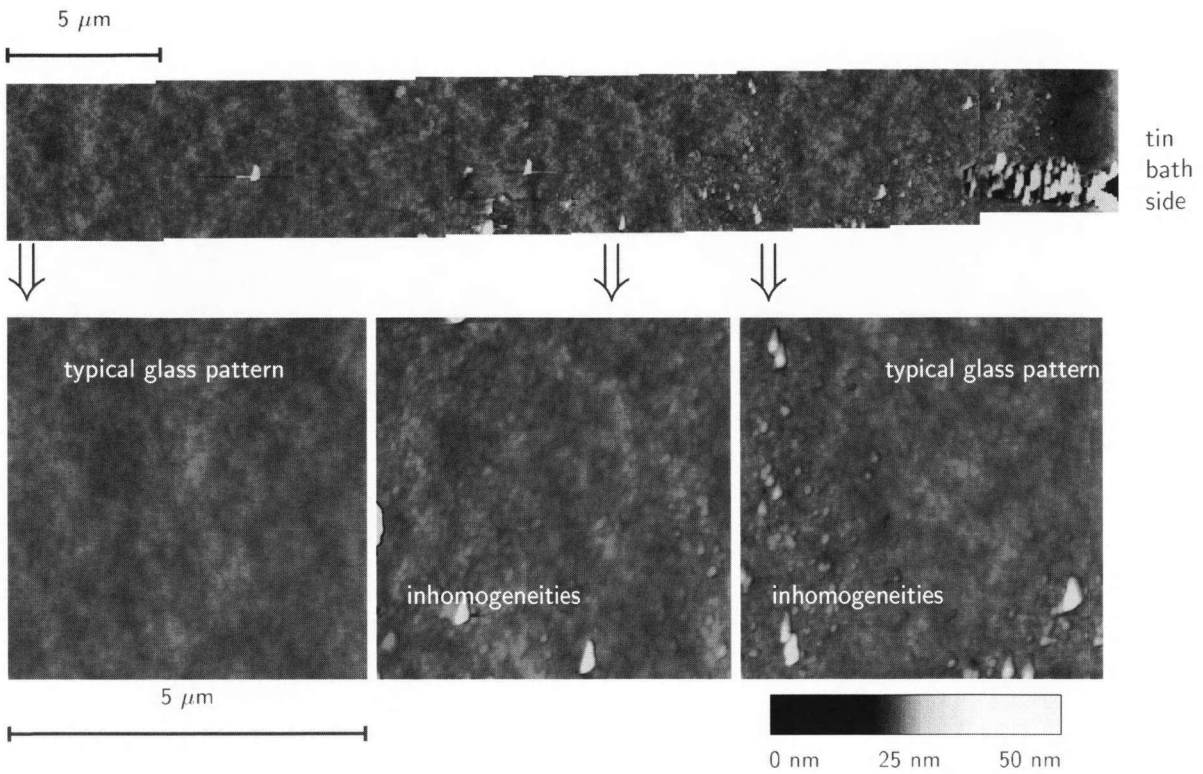

Figure 3. Sequence of AFM height mode images of various sections of a fracture surface of glass OG0605 from the edge of the tin bath side to a depth of 45 μm into the glass (from right to left) and several enlarged zooms below.

than a distinct value [8 and 9]. This Sn^{4+} acts as a network former in the glass structure [22], changing the glass properties in a superficial layer. Thus, for example, the thermal expansion coefficient α is decreased and the viscosity η increased in the melt state, whereas the glass transition temperature T_g is also increased. As a consequence, a wrinkling of the tin bath glass surface may occur, producing the greyish haze.

Figures 4a and b show AFM images of float glass surfaces with bloom. Figure 4a displays the bloom on the float glass D0130 of 4 mm thickness which has been annealed as a (100 × 100) mm^2 sheet for 1 h at 670 °C, followed by a cooling with the natural furnace rate. The wave pattern produced at the surface is irregular, has a wavelength of ≈ 3 μm and shows an rms roughness of 65 to 75 nm. A glass sample with the dimensions of (5 × 5) mm^2 showed a similar wave pattern, however, with a smaller rms roughness of 50 to 60 nm. On the other hand, a rectangular sample with the dimensions of (20 × 100) mm^2, which had been annealed simultaneously with the other samples, yields two texturized orthogonally arranged wave patterns in the interior, see figure 4b. The wavelength of the pattern in x-direction is ≈ 2.4 μm, whereas that in y-direction is ≈ 13.4 μm. The wave pattern at the edge still is texturized, however, there is only one type of wave present parallel to the edge of the longer side with a wavelength of ≈ 3 μm. Moreover, there is also a strong influence of the temperature/time regime on the occurrence of bloom. Reducing the holding time at 650 °C from 1 to 0.5 h yields a surface whose roughness is only half of that at the longer time, and a very rapid cooling after 0.5 h or a heating to 650 °C only, followed by a cooling with the natural furnace rate, resulted in no bloom at all [10]. An annealing under reducing conditions did not yield bloom, similar to what had been found earlier [1, 23 and 24].

The borofloat glasses investigated did not show bloom, which coincides with the findings of Schneider et al. [25]. Within this work bloom could be evidenced only on the surfaces of the white soda-lime silicate float glasses with a low Fe_2O_3 content (OW0017, OF0115, D0130, see table 1), whereas the green (OG0605, V1800) and blue (BG0560) float glasses with higher Fe_2O_3 contents did not develop bloom under any condition. Williams et al. [9] reported a similar tendency, and this circumstance was also confirmed from an industrial point of view [26]. How can this be explained?

Within the joint-laboratory project "Tin in float glass" we precisely measured the in-depth profiles of all relevant species in the nanometer and the micrometer regions of different float glasses [7] and also the in-depth profile of the Sn^{2+}/Sn^{4+} ratio [27]. One important result, described in detail in [28], shows that the tin in-depth profiles of the float glasses investigated are quite different in the first 100 nm from the surface. Whereas the silicate float glasses with low Fe_2O_3 contents display

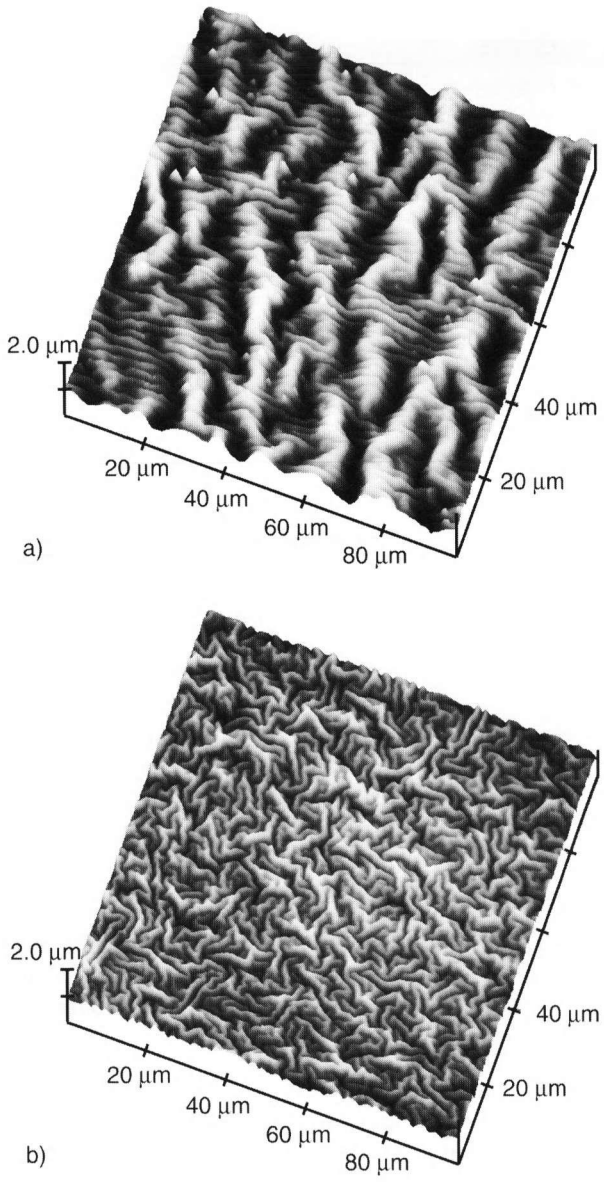

Figures 4a and b. Float glass D0130 showing bloom after annealing for 1 h at 650 °C in air; a) AFM height mode image in the middle of a (100 × 100) mm^2 sized sample, b) AFM height mode image in the middle of a (20 × 100) mm^2 sized sample.

SnO_2 surface concentrations up to 7 wt% and a steep gradient in these profiles, the SnO_2 profiles of the borofloat and the silicate float glasses with high Fe_2O_3 contents have lower surface concentrations (< 2.4 wt%) and a much smoother decrease from the surface to the bulk. After annealing these float glasses in air this tendency becomes even stronger. Thus, for example, the SnO_2 concentration of the Fe_2O_3-poor silicate float glass OW0017 is increased from ≈ 6.2 to ≈ 29 wt% at its maximum 30 nm below the surface after annealing for 1 h at 650 °C in air. This also makes the SnO_2 gradient near the surface very steep. On the other hand, the mentioned annealing step smoothens the SnO_2 profile of the Fe_2O_3-rich V1800 float glass [28]. Similar results are expressed by figure 5, which shows tin profiles of the other float glasses after annealing for 1 h at 650 °C. The analyses by secondary neutral mass spectrometry (SNMS) were obtained under similar conditions to those reported in [28]. Thus, one can conclude that during annealing in air a tin species is forced to diffuse from the interior to the surface in the case of the silicate float glasses with low Fe_2O_3 contents, whereas a diffusion process in the opposite direction obviously takes place in the case of the glasses with the high Fe_2O_3 contents.

When a glass melt, which has been prepared under oxidizing conditions, enters the strongly reducing float chamber, a very strong and rapid change occurs in its oxidation state near the surface. At the tin bath side this causes the redox process [7]

$$2Fe^{3+} + 3O^{2-} + Sn^0 \leftrightarrow 2Fe^{2+} + 2O^{2-} + SnO. \quad (1)$$

The Fe^{2+} ions produced in this way enable the penetration of Sn^{2+} ions into the glass melt by an ion exchange process. Since the total number of Fe^{2+} ions is very low in the case of glass OW0017, only a small part of these Sn^{2+} ions can diffuse into the glass. As a consequence a steep tin (mainly Sn^{2+}) gradient is formed near the surface. In the case of glass V1800 the total number of Fe^{2+} ions is high. This enables a far-reaching penetration of Sn^{2+} ions into the glass melt. A gradient in tin concentration does not occur near the surface, however, this glass tends to form an anomalous tin (Sn^{4+}) hump in the micrometer region [7].

When glass OW0017 is annealed in air, most of the Sn^{2+} ions near the surface are oxidized to Sn^{4+} and a Sn^{2+} depletion occurs there. This now causes an opposite gradient in the Sn^{2+} concentration with the consequence of a reversed Sn^{2+} diffusion from the interior to the surface. When reaching the surface region these Sn^{2+} ions are also oxidized to Sn^{4+}, finally forming a very high and steep tin (Sn^{4+}) hump near the very surface. Since the Sn^{4+} ions act as network formers in the glass structure [22], they are highly immobile. When glass V1800 is annealed in air, the Sn^{2+} ions near the surface are also oxidized to Sn^{4+}. However, the concentration of Sn^{2+} ions there is low and there is also no steep gradient. Moreover, since also the Sn^{4+} hump in the micrometer region is formed, obviously most of the Sn^{2+} ions are trapped there as Sn^{4+} and a specific tin enrichment near the surface is unlikely. A tin diffusion process from the interior to the surface was also found by [1, 15 and 24].

The other silicate float glasses behave during floating and air annealing in accordance with their Fe_2O_3 contents. Thus the glasses OF0115 and D0130 display the formation of bloom but a micrometer tin hump cannot be observed. The green glass , OG0605 shows —despite its high Fe_2O_3 content of 0.605 wt% – a tin profile similar to the tin profiles of the low Fe_2O_3 float glasses [28]. However, after an appropriate annealing of this glass in air its tin profile is smoothened similar to the profiles in

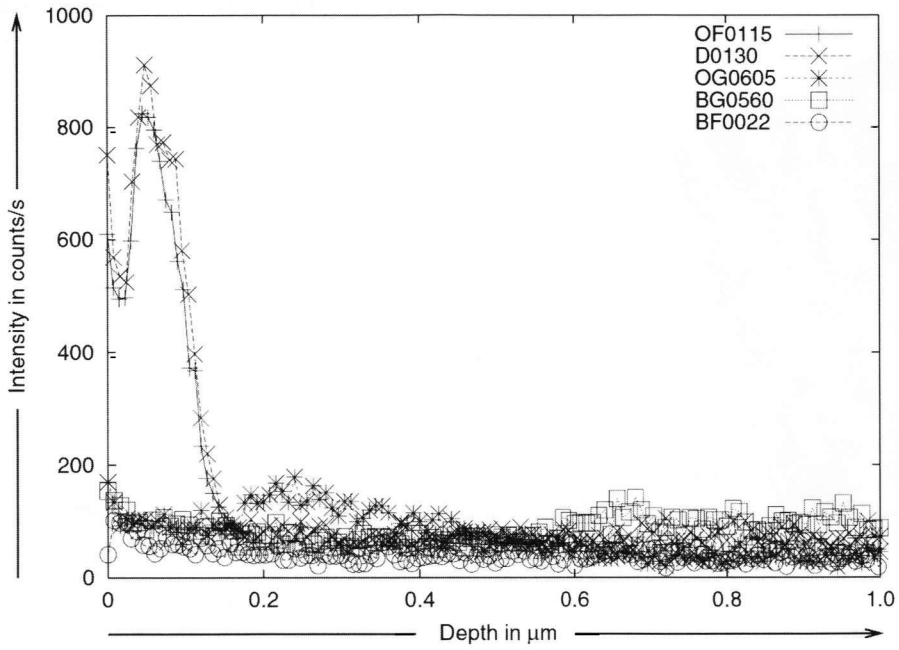

Figure 5. SNMS tin in-depth profiles of different float glasses after annealing them for 1 h at 650 °C in air.

the other float glasses with high Fe_2O_3 contents. Bloom is not formed but the glass displays the tin (Sn^{4+}) hump in the micrometer region [7]. Obviously also in this case most of the Sn^{2+} ions diffuse into that part of the glass and are trapped there as Sn^{4+} ions. The blue glass BG0560 has been manufactured under reducing conditions, which means that most of the iron ions are present as Fe^{2+} from the very beginning (see table 1). Sn^{2+} ions thus can diffuse far-reaching into the glass melt and a steep tin gradient does not form at the surface [28]. Bloom is therefore not formed there and a tin (Sn^{4+}) hump in the micrometer region has also not been found. For its formation a certain concentration of Fe^{3+} ions is necessary, which is not the case in this float glass melted in reducing conditions [7].

3.3 Model for the bloom effect

The experimental results described lead to the following conclusions:

- Using the Appen method [29] one can calculate a thermal expansion coefficient α of $9.2 \cdot 10^{-6}\,K^{-1}$ for the interior of the Fe_2O_3-poor float glass OW0017. Taking into account the SnO_2 content of 6.5 wt% at the bath side, one obtains an α value of $8.9 \cdot 10^{-6}\,K^{-1}$ for a superficial glass layer of 75 nm thickness. After annealing this glass for 1 h at 650 °C in air, one obtains under the condition of an average SnO_2 content of 22.4 wt% an α value of $8.0 \cdot 10^{-6}\,K^{-1}$ for a surface layer of 60 nm thickness. Thus the difference in the thermal expansion coefficients $\Delta\alpha$ between interior and surface increases from $0.3 \cdot 10^{-6}\,K^{-1}$ in the case of the as-received to $1.2 \cdot 10^{-6}\,K^{-1}$ for the air-annealed float glass.
- For the Fe_2O_3-rich glass V1800 a similar estimation leads to an α value of $9.6 \cdot 10^{-6}\,K^{-1}$ for the interior and to α of $9.5 \cdot 10^{-6}\,K^{-1}$ for the surface region with 2.2 wt% SnO_2. For this glass $\Delta\alpha$ is nearly negligible between surface and interior.

Similar conclusions can be drawn for the Fe_2O_3-poor float glasses OF0115 and D0130 with a high mismatch in thermal expansion between surface and interior and for the Fe_2O_3-rich glasses OG0605 and BG0560 where the thermal expansion does not change much.

There are some papers displaying similar arguments. Thus Deubener et al. [30] prepared model glasses comparable to float glass containing 5 wt% SnO_2/SnO under oxidizing and reducing conditions, respectively. The T_g values of these glasses were 586 and 576 °C and the α values at 350 to 500 °C were $10.7 \cdot 10^{-6}\,K^{-1}$ (oxidized glass) and $11.3 \cdot 10^{-6}\,K^{-1}$ (reduced glass). The authors concluded that in the case of a real float glass the SnO-containing bulk glass contracts more than the oxidized predominantly SnO_2-containing surface layer, which then leads to the formation of bloom by a wrinkling of the surface at temperatures near T_g. Le Bourhis [31] also prepared a model glass with 12.9 wt% SnO_2 and obtained an α value of $8.3 \cdot 10^{-6}\,K^{-1}$ at 20 to 300 °C. For a standard SnO_2-free soda-lime-silicate glass he measured $8.9 \cdot 10^{-6}\,K^{-1}$. Both the viscosities and the T_g values were higher for the SnO_2-containing glass, too, and the Young's moduli E amounted to 78.8 and 71.5 GPa. Poisson's ratios μ were obtained to be 0.22 and 0.21, respectively. Williams et al. [9] also determined higher viscosities and T_g values at the float glass surface compared to the bulk glass.

Le Bourhis [31] used the data determined to estimate the stress σ_T obtained during a temperature change ΔT

$$\sigma_T \approx \frac{E \cdot \alpha}{1 - \mu} \Delta T = \varphi \cdot \Delta T \tag{2}$$

where φ is a prefactor of this transient or residual stresses, and obtained $\varphi = 0.83$ MPa/K for the SnO_2-containing and 0.80 MPa/K for the SnO_2-free glass, with $\Delta\varphi = 0.03$ MPa/K. Applying a calculation method used in thin film technology [32], one obtains

$$\sigma_T = E_{\text{film}} \cdot (\alpha_{\text{film}} - \alpha_{\text{substrate}}) \cdot \Delta T \tag{3}$$

with

$$\Delta\varphi = E_{\text{film}} \cdot (\alpha_{\text{film}} - \alpha_{\text{substrate}}) \tag{4}$$

for Le Bourhis' glasses $\Delta\varphi \approx 0.05$ MPa/K, in reasonable agreement with the just calculated value.

Applying equation (4) to glass OW0017 and using Le Bourhis' E values, one obtains $\Delta\varphi = 0.02$ and 0.09 MPa/K for the as-received and the air-annealed float glasses, respectively. With equation (3) one gets for a temperature difference of $\Delta T = 500$ K a stress value at the surface of $\approx$ 10 MPa for the as-received and $\approx$ 45 MPa for the air-annealed float glasses. Since the compressive strength of normal glasses is around 1000 MPa and the tensile strength around 100 MPa [33], a failure of the glass during cooling or even a spalling between interior and surface is not yet to be expected.

A further aspect to be considered with respect to the occurrence of bloom is the low thickness of the high-SnO_2 containing superficial layer of the glass. Depending on the conditions of the thermal treatment in air it lies between about 50 and 150 nm only. In our opinion this plays an important role related to the buckling of the surface layer, which is not a stress but a stability problem [34]. A component may fail even if the stress does not surpass its strength.

One can calculate the free buckling length l for the simplifying conditions:

a) the SnO_2-containing superficial layer is treated independently of the bulk of the glass and the main buckling forces are parallel to the surface;

b) the free clamping length is identical to the free buckling length l (elastic buckling or Euler case);

c) the critical buckling stress σ_K is taken as 45 MPa, as estimated for the glass OW0017;

d) the layer thickness δ is set to 60 nm as obtained for glass OW0017;

e) the E value of 78.8 GPa is taken according to Le Bourhis [31] for the SnO_2-containing glass.

Then one gets

$$\sigma_K = \frac{\pi^2 \cdot E}{\lambda^2}, \tag{5}$$

and with a slenderness ratio λ of a rectangular cross section

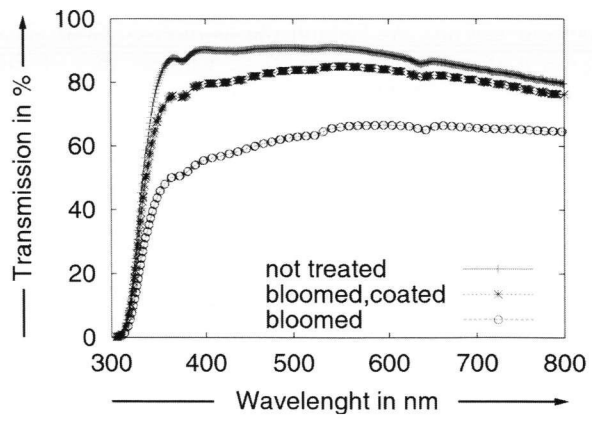

Figure 6. Comparison of optical transmission of an as-received glass, a glass showing bloom at the surface, and a glass with an SiO_2 sol-gel coating on the bloom surface.

$$\lambda = 2\sqrt{3} \cdot \frac{l}{\delta} \tag{6}$$

one obtains

$$l = \sqrt{\frac{\pi^2 \cdot E}{12\sigma_K}} \cdot \delta\,. \tag{7}$$

Inserting the data yields an estimate for the free buckling length $l \approx 2.3$ µm. This value is in reasonable agreement with the experimental data, see section 3.2. The bloom amplitudes of the surface waves between 50 to 250 nm are also not unreasonable compared to the layer thickness of 50 to 150 nm.

The σ_K value of 45 MPa for glass OW0017 was obtained for $\Delta T = 500$ K. That means that the buckling of the glass occurs at temperatures $< T_g$, too. However, since the layer in concern has a thickness of several 10 nm only, this seems also not unreasonable.

In conclusion, bloom is expected to occur on Fe_2O_3-poor glasses only, where after annealing in air a high-SnO_2 enriched surface layer exists. Fe_2O_3-rich glasses do not fulfil the conditions necessary for a buckling of the glass surface as described.

3.4 Coating of bloom surfaces

A D0130 glass substrate with the dimensions (100 × 100) mm^2 was annealed for 1 h at 670 °C (heating rate 10 K/min) and then cooled with the normal cooling rate of the furnace. The glass surfaces showed a pronounced bloom effect with an rms roughness of $\approx$ 75 nm and maximum height difference $R_{max} \approx 350$ nm. As described in section 2.1, this glass substrate was coated by an SiO_2 sol-gel coating using the dip-coating technique [10]. The withdrawal speed was 1 mm/s. The coated sample was heated at 8 K/min to 500 °C and then cooled without further annealing. The coated part of the substrate showed an rms roughness of $\approx$ 40 nm and an R_{max} < 300 nm. Figure 6 displays a comparison of the optical

transmission spectra in the wavelength region between 300 and 820 nm. At 550 nm the as-received float glass shows a transmission of ≈ 92 %, whereas that of the glass surface with bloom is decreased to ≈ 65 %. The SiO_2 sol-gel coating, which on the one hand fills up the surface waves but possibly also acts as an antireflection coating [35], increases the transmission to ≈ 85 %. Optimization of the sol-gel coating possibly might further enhance the transmission.

4. Conclusions

Eight commercial float glasses were investigated, two borofloat and six soda-lime-silicate float glasses. With high-resolution AFM the irregular ripple pattern of the as-received atmosphere and tin bath side surfaces were measured as well as also the topographies of fracture surfaces. Inhomogeneities like precipitates, crystals, phase separation or pores, caused by the in-diffusion of tin into float glass, could not be evidenced. After annealing the float glasses in air several of them showed bloom, which produces a greyish haze. The borofloat glasses and the silicate float glasses with a high Fe_2O_3 content (> 0.5 wt%) did not develop bloom, whereas the Fe_2O_3-poor glasses displayed – depending on sample size and annealing conditions – a pronounced bloom effect. In-depth analysis of the glasses showed that in the case of the Fe_2O_3-poor silicate float glasses a reversed Sn^{2+} diffusion from the interior to the surface occurs, forming there a very high and steep tin (Sn^{4+}) hump. In analogy to thin film technology a simplified model was set up and a free buckling length of ≈ 2.3 µm could be estimated for the bloom surface. This value is in reasonable agreement with the experiment. A sol-gel-derived SiO_2 coating on the bloom surface enhanced the optical transmission of the glass considerably.

*

These investigations were performed with the kind support of the Arbeitsgemeinschaft industrieller Forschungsvereinigungen (AiF), Köln (AiF-No. 11460 N), under the auspices of the Hüttentechnische Vereinigung der Deutschen Glasindustrie (HVG), Frankfurt/M., utilizing resources provided by the Bundesminister für Wirtschaft, Bonn. Thanks are due to all these institutions.

The authors also acknowledge the float glass samples provided by Dr. J. Bretschneider, Pilkington Flachglas AG, Weiherhammer; Dr. A. Kasper, Saint-Gobain Glass Deutschland GmbH, Herzogenrath; und Dr. K. Bange, Schott Glas, Mainz. The authors also gratefully acknowledge many discussions with PD Dr.-Ing. habil. Edda Rädlein, now with Universität Bayreuth, and Dr.-Ing. Constanze Müller-Fildebrandt, now with dmc^2, Hanau.

5. References

[1] Pantano, C. G.; Bojan, V; Verità, M. et al.: Tin profiles in the bottom surface of float glass: Manufacturing and heat treatment effects. In: Fundamentals of Glass Science and Technology, 1993. Proc. 2nd Conf. European Society of Glass Science and Technology, Venice 1993. Murano-Venice: Stazione Sperimentale del Vetro, 1993. p. 285–290.

[2] Franz, H.: Ion exchange and redox reactions in the float bath. Glastech. Ber. Glass Sci. Technol. **68 C1** (1995) p. 15–20.

[3] Verità, M.; Geotti-Bianchini, F.; Guadagnino, E. et. al.: Chemical characterization of the bottom side of green float glasses. Glastech. Ber. Glass Sci. Technol. **68 C1** (1995) p. 251–258.

[4] Wang, T.-J.: Penetration of tin in the surface of float glass. Glass Technol. **38** (1997) p. 104–106.

[5] Williams, K. F. E.; Johnson, C. E.; Greengrass, J. et al.: Tin oxidation state, depth profiles of Sn^{2+} and Sn^{4+} and oxygen diffusivity in float glass by Mössbauer spectroscopy. J. Non-Cryst. Solids **211** (1997) p. 164–172.

[6] Williams, K. F. E.: Johnson, C. E.; Nikolov, O. et al.: Characterization of tin at the surface of float glass. J. Non-Cryst. Solids **242** (1998) p. 183–188.

[7] Heide, G.; Müller-Fildebrandt, C.; Moseler, D. et al.: Tin in float glass: A diffusion-reaction model based on surface analysis explains the tin hump. Glastech. Ber. Glass Sci. Technol. **73 C2** (2000) p. 321–330.

[8] Pilkington, L. A. B.: The float glass process. Proc. Royal Soc., London **A 314** (1969) p. 1–25.

[9] Williams, K. F. E.; Thomas, M. R; Greengrass, J. et al: The effect of tin on some physical properties of the bottom surface of float glass and the origin of bloom. Glass Technol. **40** (1999), p. 103–107.

[10] Moseler, D.: Rasterkraftmikroskopische Untersuchungen von Floatgläsern und des Bloom-Effekts. TU Clausthal, PhD thesis 2001.

[11] Rädlein, E.; Frischat, G. H.: Atomic force microscopy as a tool to correlate nanostructure to properties of glasses. J. Non-Cryst. Solids **222** (1997) p. 69–82.

[12] Schmitz, R.; Frischat, G. H.; Paulus, H. et al.: On the quantification of SNMS analyses of silicate glasses and oxide coatings. Fresenius J. Anal. Chem. **358** (1997) p. 42–46.

[13] Moseler, D.: Erfassung der Veränderung einer Floatglasoberfläche durch Wasser mittels hochauflösender Analysenmethoden. TU Clausthal, MS thesis 1998.

[14] Kerkhof, F: Bruchvorgänge in Gläsern. Frankfurt/M.: Verl. Deutsch. Glastech. Ges., 1970.

[15] Takeda, S.; Akiyama, R.; Hosono, H.: Formation of nanometer-sized SnO_2 colloids and change in Sn-depth concentration profile in float glass induced by oxygen diffusion from atmosphere at temperatures above T_g. J. Non-Cryst. Solids **281** (2001) p. 1–5.

[16] Watanabe, Y.; Nakamura, Y.; Dickinson, J. T. et al.: Changes in air-exposed fracture surfaces of silicate glasses observed by atomic force microscopy. J. Non-Cryst. Solids **177** (1994) p. 9–25.

[17] Curtin Carter, M. M.; McIntyre, N. S.; King, H. W. et al.: The aging of silicate glass surfaces in humid air. J. Non-Cryst. Solids **220** (1997) p. 127–138.

[18] Goß, A.; Poggemann, J.-F.; Rädlein, E. et al.: Rasterkraftmikroskopie in verschiedenen Medien am Beispiel Floatglas. Poster contribution at 72nd Annual Meeting of the German Society of Glass Technology (DGG) in Münster (Germany) on 25 and 26 May 1998. (see Abstract Booklet of Meeting, p. 21–24).

[19] Rädlein, E.: Werkstoffkundliche Beurteilung von Gläsern und Schichten mittels Rastersondenmikroskopie. TU Clausthal, Habilitation thesis 1999.

[20] Gupta, P. K.; Inniss, D.; Kurkjian, C. R. et al.: Nanoscale roughness of oxide glass surfaces. J. Non-Cryst. Solids **262** (2000) p. 200–206.

[21] Rädlein, E.; Wünsche, C.; Frischat, G. H.: Atomic force microscopy investigations on vitreous coatings and glass fracture surfaces. In: Proc. XVII International Congress on

Glass, Beijing 1995. Vol. 4. Beijing: Chinese Ceram. Soc. 1995. p. 3–8.
[22] Bent, J. F.; Hannon, A. C.; Holland D. et al.: The structure of tin silicate glasses. J. Non-Cryst. Solids **232–234** (1998) p. 300–308.
[23] Hueber, B.: Zur Ursache des Auftretens von Bloom an der Floatglasoberfläche. TU Clausthal, MS thesis 1994.
[24] Laube, M.; Rauch, F.: Temperature-induced changes in the composition of float glass. Fresenius J. Anal. Chem. **353** (1995) p. 408–412.
[25] Schneider, K.; Lautenschläger, G.; Kloss, T. et al.: Microfloat technology – a new challenge for the production of high tech borosilicate flat glasses. Glastech. Ber. Glass Sci. Technol. **68 C2** (1995) p. 14–28.
[26] Kasper, A. (SAINT-GOBAIN Glass Deutschland GmbH, Herzogenrath): Pers. commun., 1998.
[27] Meisel, W.: Depth profile of tin in float glass – a CEMS study. Glastech. Ber. Glass Sci. Technol. **72** (1999) p. 291–294.
[28] Müller-Fildebrandt, C.: Wechselwirkung zwischen Zinnschmelze und Floatglas. TU Clausthal, PhD thesis 2000.
[29] Scholze, H.: Glas: Natur, Struktur und Eigenschaften. 3rd ed.. Berlin et al.: Springer, 1988. pp. 175.
[30] Deubener, J.; Brückner, R.; Hessenkemper, H.: Nucleation and crystallization kinetics on float glass surfaces. Glastech. Ber. **65** (1992) p. 256–266.
[31] Le Bourhis, E.: Tin influence on physical properties of silico-soda-lime glass. XVIII International Congress on Glass, San Francisco, CA 1998. p. P01–136. (Only available on CD-ROM from The American Ceramic Society.)
[32] Frey, H.; Kienel, G. (eds.): Dünnschichttechnologie. Düsseldorf: VDI, 1987.
[33] See [29], pp. 240.
[34] Böge, A.: Mechanik und Festigkeitslehre. Braunschweig: Vieweg, 1990.
[35] Helsch, G.; Rädlein, E.; Frischat, G. H.: On the origin of the aging process of porous SiO_2 antireflection coatings. J. Non-Cryst. Solids **265** (2000) p. 193–197.

E402P002

Contact:

Prof. Dr. G. H. Frischat
Technische Universität Clausthal
Institut für Nichtmetallische Werkstoffe, Professur für Glas
Zehntnerstraße 2a
D-38678 Clausthal-Zellerfeld

E-mail: guenther.frischat@tu-clausthal.de